

University of Wollongong

Research Online

Australian Institute for Innovative Materials -
Papers

Australian Institute for Innovative Materials

1-1-2014

A new strategy for integrating abundant oxygen functional groups into carbon felt electrode for vanadium redox flow batteries

Ki Jae Kim

Korea Electronic Technology Institute

Seung-Wook Lee

Korea Electronics Technology Institute (KETI)

Tae-eun Yim

Korea Electronics Technology Institute (KETI)

Jae-Geun Kim

University of Wollongong, Korea Electronics Technology Institute (KETI), jgk884@uow.edu.au

Jang Wook Choi

Korea Advanced Institute of Science and Technology

See next page for additional authors

Follow this and additional works at: <https://ro.uow.edu.au/aiimpapers>



Part of the [Engineering Commons](#), and the [Physical Sciences and Mathematics Commons](#)

Research Online is the open access institutional repository for the University of Wollongong. For further information contact the UOW Library: research-pubs@uow.edu.au

A new strategy for integrating abundant oxygen functional groups into carbon felt electrode for vanadium redox flow batteries

Abstract

The effects of surface treatment combining corona discharge and hydrogen peroxide (H₂O₂) on the electrochemical performance of carbon felt electrodes for vanadium redox flow batteries (VRFBs) have been thoroughly investigated. A high concentration of oxygen functional groups has been successfully introduced onto the surface of the carbon felt electrodes by a specially designed surface treatment, which is mainly responsible for improving the energy efficiency of VRFBs. In addition, the wettability of the carbon felt electrodes also can be significantly improved. The energy efficiency of the VRFB cell employing the surface modified carbon felt electrodes is improved by 7% at high current density (148 mA cm⁻²). Such improvement is attributed to the faster charge transfer and better wettability allowed by surface-active oxygen functional groups. Moreover, this method is much more competitive than other surface treatments in terms of processing time, production costs, and electrochemical performance.

Keywords

integrating, electrode, vanadium, redox, flow, batteries, abundant, oxygen, functional, groups, into, carbon, strategy, felt

Disciplines

Engineering | Physical Sciences and Mathematics

Publication Details

Kim, K., Lee, S., Yim, T., Kim, J., Choi, J., Kim, J., Park, M. & Kim, Y. (2014). A new strategy for integrating abundant oxygen functional groups into carbon felt electrode for vanadium redox flow batteries. Scientific Reports, 4 6906-1-6906-6.

Authors

Ki Jae Kim, Seung-Wook Lee, Taeun Yim, Jae-Geun Kim, Jang Wook Choi, Jung Ho Kim, Min-Sik Park, and Young-Jun Kim



OPEN

CONFERENCE
PROCEEDINGSACSMS2014
.....SUBJECT AREAS:
ELECTROCATALYSIS
BATTERIESReceived
22 August 2014Accepted
13 October 2014Published
4 November 2014

Correspondence and
requests for materials
should be addressed to
M.-S.P. (parkms@keti.
re.kr) or Y.-J.K. (yjkim@
keti.re.kr)

A new strategy for integrating abundant oxygen functional groups into carbon felt electrode for vanadium redox flow batteries

Ki Jae Kim¹, Seung-Wook Lee¹, Taeun Yim¹, Jae-Geun Kim¹, Jang Wook Choi², Jung Ho Kim³, Min-Sik Park¹ & Young-Jun Kim¹

¹Advanced Batteries Research Center, Korea Electronics Technology Institute, Seongnam Gyeonggi 463-816, Republic of Korea,

²Graduate School of Energy, Environment, Water, and Sustainability (EEWS), Korea Advanced Institute of Science and Technology (KAIST), 291 Daehakro, Yuseong-gu, Daejeon 305-701, Republic of Korea, ³Institute for Superconducting and Electronic Materials, University of Wollongong, Innovation Campus, North Wollongong, New South Wales 2500, Australia.

The effects of surface treatment combining corona discharge and hydrogen peroxide (H₂O₂) on the electrochemical performance of carbon felt electrodes for vanadium redox flow batteries (VRFBs) have been thoroughly investigated. A high concentration of oxygen functional groups has been successfully introduced onto the surface of the carbon felt electrodes by a specially designed surface treatment, which is mainly responsible for improving the energy efficiency of VRFBs. In addition, the wettability of the carbon felt electrodes also can be significantly improved. The energy efficiency of the VRFB cell employing the surface modified carbon felt electrodes is improved by 7% at high current density (148 mA cm⁻²). Such improvement is attributed to the faster charge transfer and better wettability allowed by surface-active oxygen functional groups. Moreover, this method is much more competitive than other surface treatments in terms of processing time, production costs, and electrochemical performance.

Vanadium redox flow batteries (VRFBs) have received a great deal of attention as promising energy storage systems for use in large-scale applications^{1,2}. Carbon felt has been widely used for electrodes in VRFBs owing to its good chemical stability and large reactive surface area³. Low electrochemical activity and poor wettability originating from its hydrophobic nature, however, result in significant polarization and poor energy efficiency during operation. Therefore, it is desirable to develop proper surface treatments of carbon felt for full utilization of its advantages particularly for practical applications.

It has been widely accepted that surface-active oxygen functional groups are effective in catalyzing redox reactions of active species and improving the wettability of carbon felt⁴⁻⁷. In order to populate the surface of carbon felts with these functional groups, many researchers have used various surface modification techniques, including electrochemical oxidization, heat treatment, plasma treatment, and irradiation treatment⁴⁻⁶. Most of these approaches, however, suffer from long processing time, processing difficulty, and high production costs. Thus, it is necessary to develop a new, simple, and cost-effective surface modification process, allowing for the formation of abundant and robust oxygen functional groups.

Herein, we propose a new strategy to accomplish this, based on a combination of corona discharge and hydrogen peroxide (H₂O₂) treatments (Figure 1). First, a corona discharge is applied, effectively forming many instable free radicals on the carbon felt surface⁸⁻¹⁰. These free radicals are then converted to surface-active oxygen functional groups during the following H₂O₂ treatment. As a result of the modified surface properties, the new carbon felt leads to substantially improved performance of VRFBs via enhanced wetting and catalytic activity in the reaction with vanadium ions.

Results

The morphologies and microstructures of the treated carbon felt samples were examined by field-emission scanning electron microscopy (FESEM) and micro-Raman spectroscopy (Figure S1 in the Supporting Information). No noticeable structural change was observed in the carbon felt treated only with H₂O₂ (HCF)

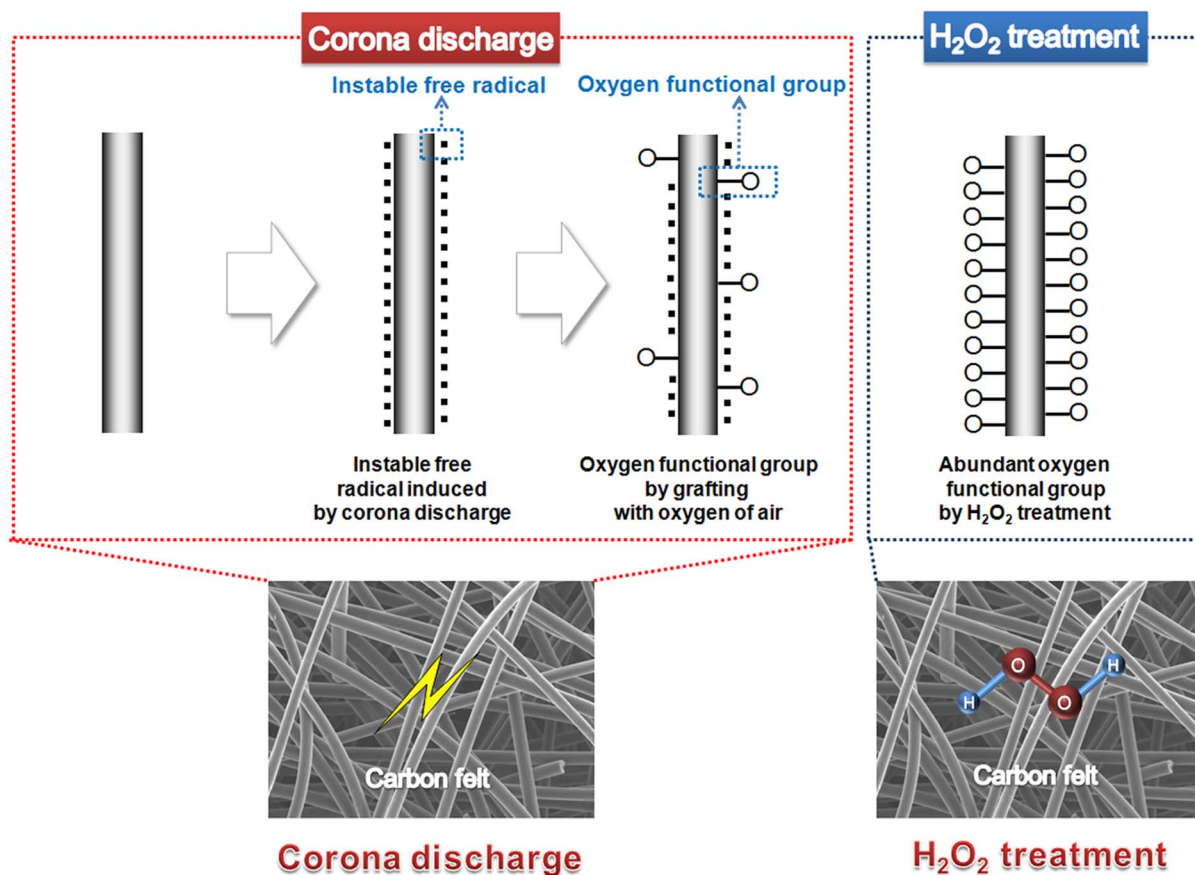


Figure 1 | Schematic illustration of the proposed treatment for integrating abundant surface-active oxygen functional groups into carbon felts. This treatment includes a corona discharge followed by sonication in H_2O_2 solution.

when compared to bare carbon felt (BCF). Additionally, no difference was observed between BCF and the carbon felt treated by corona discharge along with H_2O_2 treatment (PCF). In other words, neither corona discharge nor H_2O_2 treatment significantly affects the physical properties of carbon felt.

To further inspect the surface chemistry of the carbon felt samples, we carried out Fourier transform infrared (FT-IR) spectroscopy; the results are shown in Figure 2a. All carbon felt samples show a band at 1633 cm^{-1} , corresponding to a $\text{C}=\text{C}$ vibration¹¹. While only a weak band attributed to the presence of hydroxyl groups ($\text{C}-\text{OH}$) was observed in the region between 1240 and 900 cm^{-1} in the spectrum of BCF, two strong bands clearly indicating hydroxyl group formation ($1240\text{--}900\text{ cm}^{-1}$) and $\text{C}-\text{O}$ group ($1500\text{--}1340\text{ cm}^{-1}$) formation were observed in HCF¹¹. This demonstrates that the H_2O_2 treatment on its own was effective in integrating oxygen-based functional groups. Interestingly, PCF showed additional bands at around 1726 and 1290 cm^{-1} , which correspond to carboxyl groups (COOH) and additional $\text{C}-\text{O}$ groups, respectively¹¹. This indicates that many more oxygen functional groups were formed by using corona discharge before the H_2O_2 treatment, as was expected.

In most cases, it is nontrivial to quantify the amount of functional groups generated after the surface treatment. In order to better address this issue, tetraethylorthosilicate (TEOS) was used as a chemical indicator in a titration. TEOS is known to react quantitatively with nucleophilic oxygen functional groups, leading to the formation of orthosilicate and a method to roughly estimate the number of oxygen functional groups in a given sample^{12–14}. As expected, this method revealed no evidence for orthosilicate formation on the BCF surface (Figure 2a); however, orthosilicate formation was quite noticeable on the surfaces of HCF (Figure 2c) and PCF (Figure 2d), with a greater proportion on PCF than HCF. A new

peak at 669 cm^{-1} provides direct evidence for $\text{Si}-\text{O}$ bond formation (Figure S2)¹².

To investigate the effect of the surface treatment on the wettability of carbon felts, we measured the contact angles. The contact angle of BCF was determined to be 107.0° (Figure 2e), while that of HCF was found to be 83.1° (Figure 2f). The contact angle of carbon felt samples that underwent only corona discharge was also measured and was found to be 70.9° (Figure S4a). It was difficult, however, to measure the contact angle of PCF because it immediately became soaking wet when introduced to water (Figure 2g and S3). It seems that corona discharge pre-treatment makes the carbon felt more compatible with H_2O_2 solution during the treatment process. This suggests that the combined treatment by the corona discharge and H_2O_2 completely alters the carbon felt surface from a hydrophobic one to a hydrophilic one, positively affecting the wettability.

The electrochemical performance of the carbon felt electrodes was examined by cyclic voltammetry (CV). Based on the obtained CV curves (Figures S5 and S6), we compared the normalized peak currents and peak separations of the carbon felt electrodes for vanadium redox reactions in the catholyte and anolyte as a function of scan rate, as shown in Figure 3. The peak currents in PCF for the $\text{VO}^{2+} \leftrightarrow \text{VO}_2^+$ redox reactions in the catholyte were larger than those of BCF and HCF at all scan rates (Figure 3a), although the peak separations of PCF were not much different from those of BCF and HCF (Figure 3b). From the comparison, we found that PCF exhibited about 1.32 and 1.26 times higher oxidation and reduction peak currents, respectively, than BCF. PCF also exhibited much larger peak currents and smaller peak separations for the $\text{V}^{2+} \leftrightarrow \text{V}^{3+}$ redox reactions in the anolyte compared to BCF and HCF (Figure 3c and 3d). Note that inevitable asymmetric behaviors of anodic peak currents were still found in all carbon felt electrodes at high scan rates

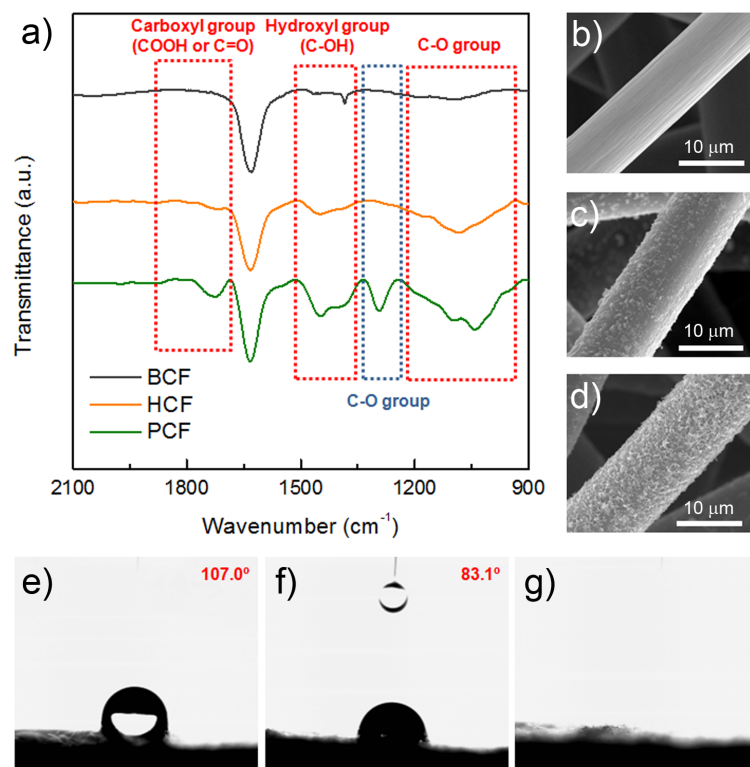


Figure 2 | Structural characterizations of BCF, HCF, and PCF: (a) Fourier transform infrared (FT-IR) spectra of BCF, HCF, and PCF. Field-emission scanning electron microscopy (FESEM) images of (b) BCF, (c) HCF, and (d) PCF after chemical titration using TEOS as a chemical indicator. Photographs of the contact angle measurements on (e) BCF, (f) HCF, and (g) PCF.

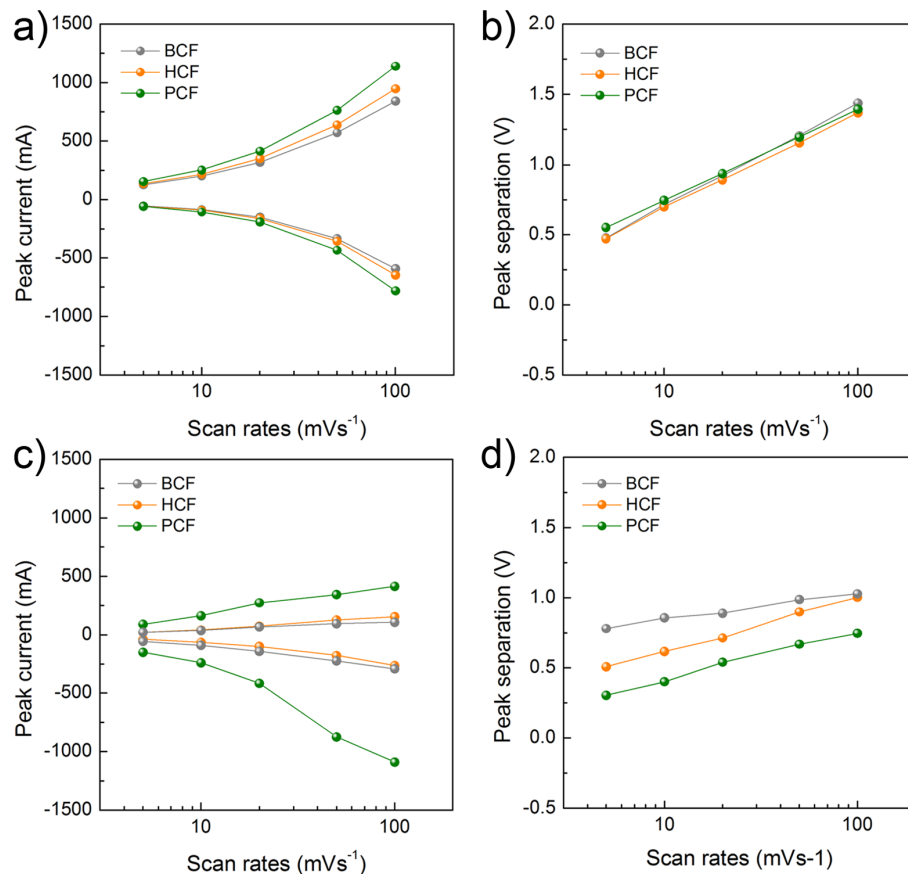


Figure 3 | Electrochemical properties of BCF, HCF, and PCF: (a) peak current and (b) peak separation for the $\text{VO}^{2+} \leftrightarrow \text{VO}_2^+$ redox reaction in catholyte; and (c) peak current and (d) peak separation for the $\text{V}^{2+} \leftrightarrow \text{V}^{3+}$ redox reaction in anolyte.

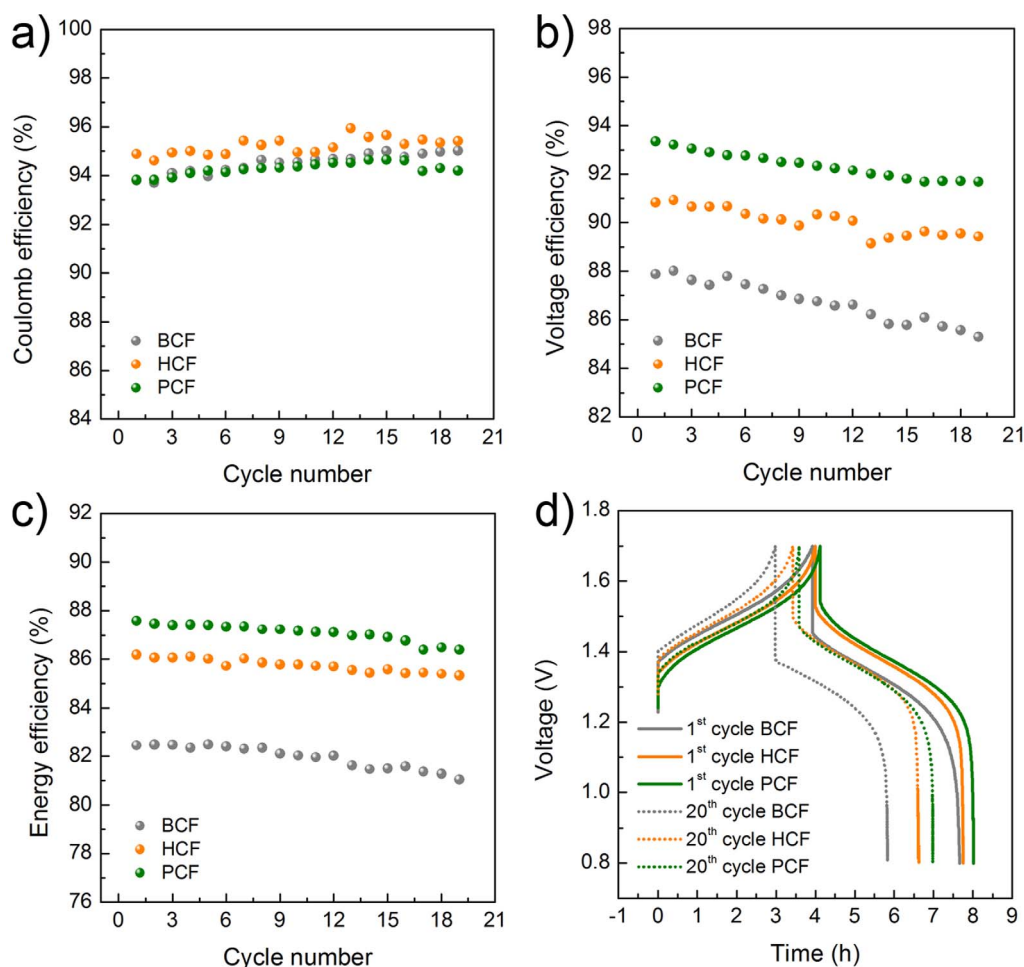


Figure 4 | Electrochemical performance of VRFB cells employing BCF, HCF, and PCF: (a) coulomb efficiency, (b) voltage efficiency, (c) energy efficiency, and (d) charge-discharge profiles for the 1st and 20th cycles.

over 50 mV s^{-1} , which might be induced by undesirable H_2 evolution¹⁵. The superior performance of PCF is attributed to the significantly improved activity and wettability of the carbon felt resulting from the increased surface-active oxygen concentrations, especially by its effects towards addressing the relatively sluggish kinetics of $\text{V}^{2+} \leftrightarrow \text{V}^{3+}$ in the anolyte¹⁶. These findings are further supported by the electrochemical impedance spectroscopy (EIS) results (Figure S7). The arc in the Nyquist plots is closely related to the charge transfer reaction at the interface between the electrolyte and the electrode. The radius of the arc reflects the charge transfer resistance, and the magnitude of the arc indicates the reaction kinetics. The semi-circle of the PCF sample is far smaller than the others, reflective of the markedly reduced activation barriers for the vanadium redox reaction.

Figure 4 shows the electrochemical performance of VRFB cells containing BCF, HCF, and PCF electrodes. Each cell was galvanostatically charged and discharged at a constant current density of 32 mA cm^{-2} for 20 cycles. The PCF cell exhibited a longer operation time (8.0 h) during the first cycle than the cell with BCF (7.6 h) under otherwise identical conditions (Figure 4a). The longer operation time of the PCF cell was still maintained after 20 cycles, with a loss of only 1.0 h, whereas the BCF cell lost 1.8 h. This suggests that the effect of the surface treatment is sustainable over cycling. Even if all the cells showed similar coulombic efficiencies of approximately 94–95% during cycling (Figure 4b), the PCF cell exhibited a remarkably improved voltage efficiency of 93.5% in the first cycle, a value that decreased only marginally to 92.0% after 20 cycles. The cell with PCF also showed the highest energy efficiency of 87.6% in the first

cycle and maintained good cycling performance in the subsequent cycles (Figure 4d). After 20 cycles, only 1.2% of the energy efficiency had decayed in the PCF cell. These improvements likely resulted from the reduction of the electrochemical polarization of the vanadium redox pairs at the electrodes, reconfirming that surface-active oxygen effectively increases the reaction kinetics of the VRFB cell by catalyzing the redox reactions without sacrificing coulombic efficiency. These trends between the cells were consistent in the CV and EIS results (Figure S7).

To investigate the rate capabilities, the cells were charged and discharged at various current densities, ranging from 32.0 to 145.8 mA cm^{-2} (Figure 5). As the applied current increased, the capacity and energy efficiency of the cells showed a tendency to decrease. Regardless of the applied current, however, the PCF cell exhibited the highest capacity and energy efficiency. For example, the PCF cell showed an energy efficiency of 68% at the high current density of 145.8 mA cm^{-2} , compared to 60% and 65% for the BCF and HCF cells, respectively. In addition, the capacity of the cell employing the PCF was 1752 mAh at a current density of 145.8 mA cm^{-2} (Figure 5d). In contrast, the capacity of the VRFB employing the BCF was 1036 mAh under the same conditions (Figure 5d). To explain such an improvement of rate capability due to PCF, we attempted to calculate the reaction rate constant, k , of the $\text{VO}^{2+} \leftrightarrow \text{VO}_2^+$ and $\text{V}^{2+} \leftrightarrow \text{V}^{3+}$ redox reactions, based on the results of cyclic voltammetry obtained at different scan rates (5 – 20 mV s^{-1}). The reaction rate constant was determined using following Equation (1)¹⁷:

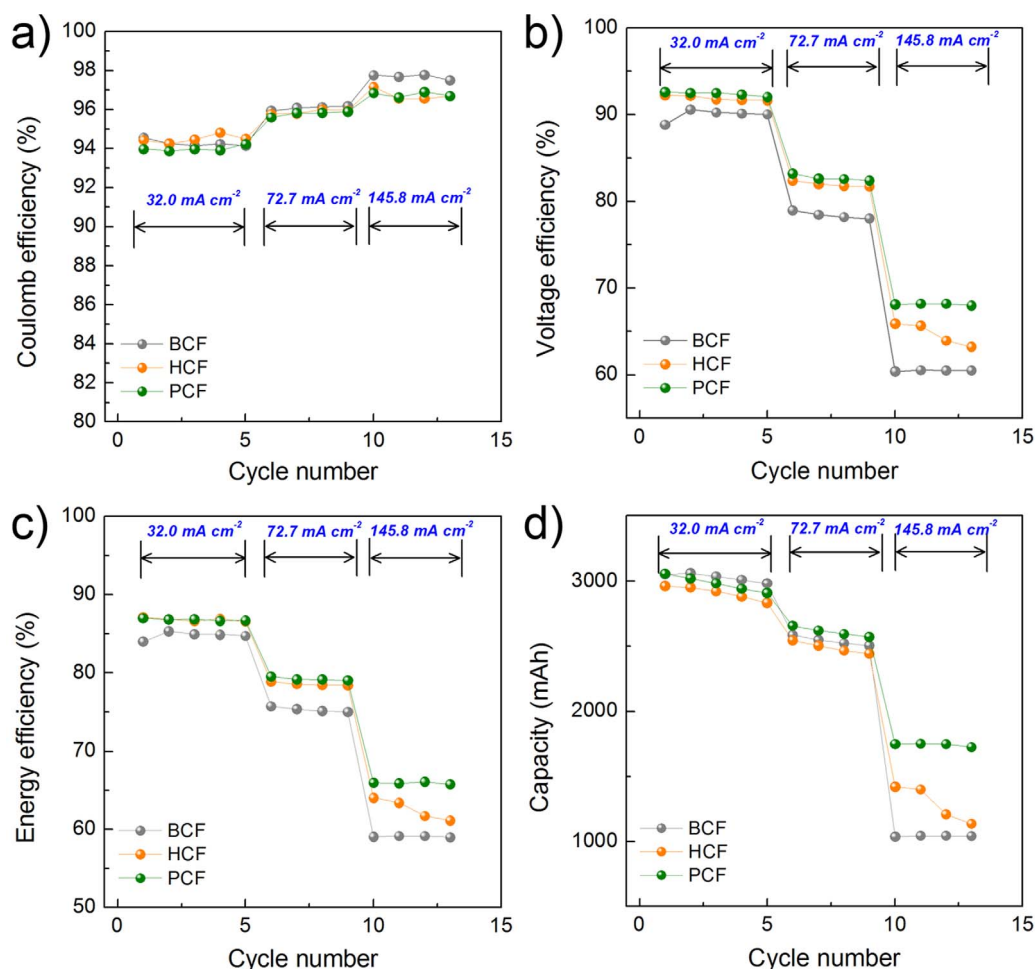


Figure 5 | Electrochemical performance of VRFB cells employing the BCF, HCF, and PCF electrodes at various current densities ranging from 32.0 to 145.8 mA cm⁻²: (a) Coulomb efficiency, (b) voltage efficiency, (c) energy efficiency, and (d) discharge capacity.

$$i_p = 0.227nFAC_0k \exp[-\alpha nF(E_p - E^0)/RT] \quad (1)$$

where i_p is the peak current, n is the number of electrons involved in the reaction, F is Faraday's constant, A is the active surface area of the electrode, C_0 is the bulk concentration of oxidant, E_p is peak potential, and E^0 is the equilibrium potential. From this equation, a plot of $\ln(i_p)$ vs. $E_p - E^0$, having a slope of $-\alpha nF/RT$ and an intercept proportional to k , can be obtained, as shown in Figure S8. The measured reaction rate constants of the BCF, HCF, and PCF for the $\text{VO}^{2+} \leftrightarrow \text{VO}_2^+$ and $\text{V}^{2+} \leftrightarrow \text{V}^{3+}$ redox reactions are summarized in Table 1. The reaction rate constant for $\text{VO}^{2+} \leftrightarrow \text{VO}_2^+$ on PCF exhibited a slightly higher value than on BCF and HCF. Interestingly, it is clearly found that PCF had a much higher reaction rate constant for the $\text{V}^{2+} \leftrightarrow \text{V}^{3+}$ redox reaction than those of BCF and HCF.

This result provides support for the effective enhancement of the sluggish kinetics of the $\text{V}^{2+} \leftrightarrow \text{V}^{3+}$ redox reaction by the proposed surface treatment. Therefore, the superior voltage efficiency of the

PCF cell can be explained by the catalytic effect of the integrated oxygen functional groups on the kinetics of the redox reactions, in particular, a sluggish $\text{V}^{2+} \leftrightarrow \text{V}^{3+}$ redox reaction in the anolyte. Based on our observations, we believe that the electrochemical activity of the carbon felt can be improved significantly by the proposed surface treatment, which leads to the improvement of cell performance, in such aspects as the voltage and energy efficiencies of the VRFBs.

Discussion

The proposed surface treatment combining corona discharge and H_2O_2 is quite effective in producing abundant surface-active oxygen functional groups on the carbon felt surfaces. By using a corona discharge pre-treatment, many instable surface free radicals can be generated on the carbon felt surface, which reacts with H_2O_2 to form the desired oxygen functional groups. After the proposed surface treatment, the electrochemical activities of the carbon felt electrodes were notably improved, exhibiting lower electrochemical polariza-

Table 1 | Reaction rate constants of BCF, HCF, and PCF electrodes for (a) $\text{VO}^{2+} \leftrightarrow \text{VO}_2^+$ redox reactions in the catholyte, and (b) $\text{V}^{2+} \leftrightarrow \text{V}^{3+}$ redox reactions in the anolyte

| Samples | Reaction rate constant, k (10^{-3} m s^{-1}) | | | |
|---------|--|--|---|---|
| | $\text{VO}^{2+} \rightarrow \text{VO}_2^+$ oxidation | $\text{VO}_2^+ \rightarrow \text{VO}^{2+}$ reduction | $\text{V}^{2+} \rightarrow \text{V}^{3+}$ oxidation | $\text{V}^{3+} \rightarrow \text{V}^{2+}$ reduction |
| BCF | 0.0098 | 0.8370 | 0.2135 | 0.0007 |
| HCF | 0.1024 | 0.9055 | 1.5290 | 0.0126 |
| PCF | 0.1030 | 1.2320 | 24.2365 | 0.5417 |



tion for vanadium redox reactions and thus resulting in superior voltage and energy efficiencies. Furthermore, in addition to improved electrochemical performance, this new method brings the additional advantage of lower production costs due to shorter processing time and easier handling as compared to other available methods. Overall, this new surface treatment is promising for both electrochemical performance and scalability and could thus be a viable option for future VRFBs.

Methods

Preparation of surface modified carbon felts. Poly(acrylonitrile) (PAN) carbon felt (3 mm thick, GF-3F, Nippon Carbon Co.) was used for both the positive and negative electrodes for the electrochemical measurements. The carbon felt was pre-treated by using an HK-2000 corona discharge instrument (HAN GOOK Hi-Frequency) with a 15 mm dielectric barrier between the electrode and the carbon felt. The front side of the carbon felt was exposed twice for 15 s, each time at ambient temperature in air and under a discharge current of 4 A, after which the other side of the carbon felt was treated under the same conditions. The resulting material was then sonicated (VCX 500, Sonics & Materials, INC.) in 30% aqueous H_2O_2 solution for 1 h at 100 W. After sonication, the carbon felt was dried under vacuum at 80°C for 12 h. The conditions for the corona discharge and H_2O_2 treatments were optimized by pre-screening the electrochemical properties using cyclic voltammetry and VRFB single cells.

Sample characterizations. The morphologies of the carbon felt electrodes were observed using a field emission scanning electron microscope (FESEM, JEOL JSM-7000F). Raman spectra were collected using a Raman spectrometer (BRUKER Senterra Grating 400) with a He-Ne laser at a wave-length of 532 nm. X-ray photoelectron spectroscopy (XPS, Thermo Scientific, Sigma Probe) was used to characterize the surface chemistry, including elemental compositions and chemical states. In addition, surface functionalities were identified using Fourier-transform infrared spectroscopy (FT-IR, Bruker VERTEX70) operating at room temperature in the $400\text{--}4000\text{ cm}^{-1}$ range. To assess the amount of oxygen-based functional groups on the carbon felt surfaces, chemical titration was performed using tetraethyl orthosilicate (TEOS , $\text{SiC}_8\text{H}_{20}\text{O}_4$, Aldrich, 98%). The bare and modified carbon felt were immersed in TEOS for 24 h. The samples were then washed with distilled water and dried at room temperature for 12 h to remove residual reagents. The contact angle measurements were carried out for each sample by the water droplet method (GSA model, Surface Technology Korea), involving the pipetting of a certain amount of de-ionized water onto the sample surface. The contact angles were determined using Surface Energy & Tension Measurement New Goniostar Contact Angle software.

Electrochemical measurements. To understand the electrochemical properties of the carbon felt electrodes, cyclic voltammetry (CV) was performed using a three-electrode glass cell, comprising the selected carbon felt electrode as the working electrode, platinum mesh as the counter electrode, and a saturated calomel electrode (SCE) as the reference electrode. The test was performed over the voltage range from -1.0 to 2.0 V vs. SCE and at scan rates ranging from 5 to 100 mV s^{-1} . The positive and negative electrolytes were 0.1 M VOSO_4 in $2.0\text{ M H}_2\text{SO}_4$ and 0.1 M V^{3+} in $2.0\text{ M H}_2\text{SO}_4$, respectively. The negative electrolyte was prepared by the electrochemical reduction of the positive electrolyte. Electrochemical impedance spectroscopy (EIS) results were obtained using a three-electrode glass cell prepared by the same method described above. AC impedance analysis was performed with a potentiostat/galvanostat (EC-Lab, Bio-Logic) over frequency values ranging from 1 MHz to 10 mHz with an amplitude of 5 mV . The applied potentials were open circuit voltage (OCV) conditions for both electrolytes.

Cell tests. The vanadium redox flow battery cells were comprised of the electrolytes, electrodes, bipolar plates (BPs), ion exchange membranes, tanks, and pumps. The electrolytes were prepared by dissolving 1.7 M VOSO_4 (Aldrich, 99.5%) in $2.5\text{ M H}_2\text{SO}_4$ solution (Aldrich, 99.9%). The electrolyte volumes were 80 mL on both sides. The treated and untreated carbon felt samples were used as the positive and negative electrodes ($5\text{ cm} \times 5\text{ cm}$). Nafion membrane (N117, Dupont) and conventional graphite bipolar plate (BP) were employed in the test cell. A potentiostat/galvanostat (EC-Lab, Bio-logic) was used for cell performance evaluation. The test cells were charged and discharged in the $1.7\text{--}0.8\text{ V}$ range at a current density of 35 mA cm^{-2} . The flow rate was fixed at 1.37 mL s^{-1} , which was controlled by the pump.

1. Ponce de Leon, C., Frias-Ferrer, A., Gonzalez-Garcia, J., Szanto, D. A. & Walsh, F. C. Redox flow cells for energy conversion. *J. Power Sources* **160**, 716–732 (2006).
2. Wang, W. *et al.* Recent progress in redox flow battery research and development. *Adv. Funct. Mater.* **23**, 970–986 (2013).

3. Kaneko, H. *et al.* Vanadium redox reactions and carbon electrodes for vanadium redox flow battery. *Electrochim. Acta* **36**, 1191–1196 (1991).
4. Sun, B. & Skyllas-Kazacos, M. Modification of graphite electrode materials for vanadium redox flow battery application-I. Thermal treatment. *Electrochim. Acta* **37**, 1253–1260 (1992).
5. Kim, K. J., Kim, Y.-J., Kim, J.-H. & Park, M.-S. The effects of modification on carbon felt electrodes for use in vanadium redox flow batteries. *Mater. Chem. Phys.* **131**, 547–553 (2011).
6. Shao, Y. *et al.* Nitrogen-doped mesoporous carbon for energy storage in vanadium redox flow batteries. *J. Power Sources* **195**, 4375–4379 (2010).
7. Li, W., Liu, J. & Yan, C. Reduced graphene oxide with tunable C/O ratio and its activity towards vanadium redox pairs for an all vanadium redox flow battery. *Carbon* **55**, 313–320 (2013).
8. Desimoni, E., Salvi, A. M., Ceipidor, U. B. & Casella, I. G. Activation of carbon fibres by negative d.c. corona discharge at ambient pressure and temperature. *J. Electron Spectrosc.* **70**, 1–9 (1994).
9. Desimoni, E., Salvi, A. M., Langerame, F. & Watts, J. F. X-ray photoelectron spectroscopy, X-ray excited Auger electron spectroscopy and time-of-flight secondary ion mass spectroscopy characterization of carbon fibres activated by d.c. corona discharge at ambient pressure and temperature. *J. Electron Spectrosc.* **85**, 179–191 (1997).
10. Park, S. J., Cho, K. S., Zaborski, M. & Slusarski, L. Filler-Elastomer interactions. 7. The effect of corona discharge treatment on surface properties and adhesion characteristics of carbon black/rubber composites. *J. Korean Ind. Eng. Chem.* **14**, 23–28 (2003).
11. Pretsch, E., Bühlmann, P. & Affolter, C. *Structure determination of organic compounds* (3rd English edition) 263–270 (Springer, Germany, 2000).
12. Yim, T. *et al.* A facile method for construction of a functionalized multi-layered separator to enhance cycle performance of lithium manganese oxide. *RSC Adv.* **3**, 25657–25661 (2013).
13. Davydov, V. Y., Kiselev, A. V. & Zhuravlev, L. T. Study of the surface and bulk hydroxyl groups of silica by infra-red spectra and D₂O-exchange. *Trans. Faraday Soc.* **60**, 2254–2264 (1964).
14. Anedda, A., Carbonaro, C. M., Clemente, F., Corpino, R. & Ricci, P. C. Raman investigation of surface OH-species in porous silica. *J. Phys. Chem. B* **107**, 13661–13664 (2003).
15. Agar, E., Dennison, C. R., Knehr, K. W. & Kumbur, E. C. Identification of performance limiting electrode using asymmetric cell configuration in vanadium redox flow batteries. *J. Power Sources* **225**, 89–94 (2013).
16. Li, B. *et al.* Bismuth Nanoparticle Decorating Graphite Felt as a High-Performance Electrode for an All-Vanadium Redox Flow Battery. *Nano Lett.* **13**, 1330–1335 (2013).
17. Bard, A. J. & Faulkner, L. R. *Electrochemical Methods-Fundamentals and Applications* (2nd edition) 222–224 (Wiley, New York, 2001).

Acknowledgments

This work was partially supported by the K-Initiative, the Energy Efficiency & Resources Core Technology Program (20132020000340) of the Korea Institute of Energy Technology Evaluation and Planning (KETEP) and the IT R&D program (Project no. 10041942, KEIT) of the Ministry of Trade, Industry, and Energy, Republic of Korea.

Author contributions

K.J.K. and M.-S.P. designed the overall experiments. T.Y., J.-G.K. and S.-W.L. analyzed FT-IR data and contributed to material characterizations by SEM. K.J.K., M.-S.P., J.W.C., J.H.K. and Y.-J.K. wrote the majority of the paper. All authors reviewed the manuscript.

Additional information

Supplementary Information accompanies this paper at <http://www.nature.com/scientificreports>

Competing financial interests: The authors declare no competing financial interests.

How to cite this article: Kim, K.J. *et al.* A new strategy for integrating abundant oxygen functional groups into carbon felt electrode for vanadium redox flow batteries. *Sci. Rep.* **4**, 6906; DOI:10.1038/srep06906 (2014).



This work is licensed under a Creative Commons Attribution-NonCommercial-NoDerivs 4.0 International License. The images or other third party material in this article are included in the article's Creative Commons license, unless indicated otherwise in the credit line; if the material is not included under the Creative Commons license, users will need to obtain permission from the license holder in order to reproduce the material. To view a copy of this license, visit <http://creativecommons.org/licenses/by-nc-nd/4.0/>